(2D+1) Pendulum Beams: Non-diffracting Optical Spatial Wavepackets that Simulate Quantum Pendulum Dynamics

Thao P. Nguyen, Valeria Rodríguez-Fajardo, and Enrique J. Galvez

Department of Physics and Astronomy, Colgate University, 13 Oak Drive, Hamilton, New York 13346, U.S.A.

ABSTRACT

The similarity between the 2D Helmholtz equation in elliptical coordinates and the Schrödinger equation for the simple mechanical pendulum inspires us to use light to mimic this quantum system. When optical beams are prepared in Mathieu modes, their intensity in the Fourier plane is proportional to the quantum mechanical probability for the pendulum. Previous works have produced a two-dimensional pendulum beam that oscillates as a function of time through the superpositions of Mathieu modes with phases proportional to pendulum energies. Here we create a three-dimensional pendulum wavepacket made of a superposition of Helical Mathieu-Gaussian modes, prepared in such a way that the components of the wave-vectors along the propagation direction are proportional to the pendulum energies. The resulting pattern oscillates or rotates as it propagates, in 3D, with the propagation coordinate playing the role of time. We obtained several different propagating beam patterns for the unbound-rotor and the bound-swinging pendulum cases. We measured the beam intensity as a function of the propagation distance. The integrated beam intensity along elliptical angles plays the role of quantum pendulum probabilities. Our measurements are in excellent agreement with numerical simulations.

Keywords: Pendulum beams, Quantum Pendulum, Mathieu Beams, Non-diffracting beams, Spatial Wavepackets

1. INTRODUCTION

The description of the natural world by mathematical structures often produces situations where disparate physical systems have the same mathematical structure. Examples abound, from the first-order differential equation describing exponential decay to the second-order differential equation describing the harmonic oscillator. This results in distinct systems following the same mathematical dynamic. The Schrödinger equation of quantum mechanics is a linear second-order differential equation that has a parallels in wave propagation, where the dynamics are also described by a similar type of differential equation, the Helmholtz equation.[1] Their application using light is particularly compelling because of the visual outcomes of observing optical phenomena. In particular, the quantum solution for the mechanical pendulum reduces to the Mathieu equation, which is also the angular Helmholtz equation expressed in elliptical coordinates, giving rise to Mathieu non-diffracting beams.

Non-diffracting beams are of much interest because they constitute light beams that do not change shape over a finite propagation distance. They arise when the light is set to satisfy the 2-dimensional (2-D) Helmholtz equation. Bessel beams were the first types of non-diffracting beams to be investigated.[2,3] When the mode is set to be circularly symmetric, the mode that appears follows a Bessel function. If the mode is set to have elliptical symmetry, then Mathieu modes are generated.[4,5] Similarly, Airy and parabolic beams are another interesting type of non-diffracting beams,[6–8] but in this case the transverse pattern shifts transversely producing an "accelerating" feature. That is, that while keeping its shape and size, the beam deflects in a parabolic trajectory as it propagates. Owing to having a radial representation in terms of Bessel functions, the Fourier transform of these beams reduces to a modulated ring. Thus, arbitrary modulations can produce exotic non-diffracting beams featuring various caustic patterns.[9]

Further author information: (Send correspondence to E.J.G.)
E.J.G.: E-mail: egalvez@colgate.edu, Telephone: 1 315 228 7205

There are other interesting variations of non-diffracting beams where the shaped pattern changes in orientation as the light propagates. Radial-Airy and Pearcey beams have the property of autofocusing.[10,11] A superposition of helical Bessel beams of opposite handedness or topological charge can produce a non-diffracting pattern that is asymmetric. If the beams are prepared to have slightly different transverse wave-vectors, results in an evolving phase that makes the pattern rotate as it propagates.[12]

In this work, we investigate the generation of a spatially-varying non-diffracting beam that follows a particular dynamic, that of the quantum pendulum, as mentioned above. The beams that simulate the pendulum, also called pendulum beams,[13] correspond to a set of solutions that have the same symmetry as the pendulum. Interestingly, the intensity modulation of the Fourier spectrum of the modes is proportional to the quantum-mechanical probability of the pendulum allowing a visual study of stationary states and wavepacket superpositions.[14,15] Of particular interest, is the preparation of the state superposition in such a way that the propagation of the mode reflects the time evolution of the quantum state. In this article, we present our preliminary results toward obtaining a one to one correspondence between the temporal dynamics of quantum superpositions and the propagation of the wave dynamics of the pendulum modes.

The article is organized as follows. In Sec. 2, we present the theoretical rationale behind the work, and in Sec. 3 we describe our experimental method. Section 4 presents preliminary results of our investigations.

2. THEORY

The quantization of the mechanical pendulum results in the Mathieu equation[16]

$$\frac{d^2\psi}{d\chi^2} + (a - 2q\cos 2\chi)\psi = 0\,, \tag{1}$$

where ψ is the wavefunction for the pendulum of length l and mass m, and

$$\chi = \frac{\theta}{2} \tag{2}$$

with θ the pendulum angle, being $\theta = 0$ the angle of the pendulum at the lowest position. The potential energy of the pendulum is given by

$$V = mgl(1 - \cos\theta)\,, \tag{3}$$

where g is the acceleration of gravity. A constant in the problem is the scaled potential barrier (i.e. when the pendulum is in the inverted position):

$$q = \frac{2mgl}{E_0}\,, \tag{4}$$

where $E_0 = \hbar^2/(2ml^2)$ is an energy unit.[17] The quantity a in Eq. 1 is the eigenvalue solution. The solutions are expressed in terms of their parity. The allowed scaled energies $\varepsilon = E/E_0$ of the pendulum become

$$\varepsilon_{n,e} = \frac{a_n}{4} + \frac{q}{2}, \quad \text{even}\,, \tag{5}$$

$$\varepsilon_{n,o} = \frac{b_n}{4} + \frac{q}{2}, \quad \text{odd}\,, \tag{6}$$

where $n \in \mathbb{Z}^+$ is the quantum number, with $n = 0$ allowed only for the even parity. As presented previously,[18] the solution of the 2-dimensional Helmholtz equation in elliptical coordinates also leads to the Mathieu equation. In this case, the radial and angular coordinates, ξ and χ, respectively, are related to the Cartesian coordinates, x and y, by

$$x = e\cosh\xi\cos\chi\,, \tag{7}$$

$$y = e\sinh\xi\sin\chi\,. \tag{8}$$

where e specifies the distance from the foci to the origin. Points of constant ξ and χ form confocal ellipses and hyperbolas, respectively, as shown in Fig. 1(a).

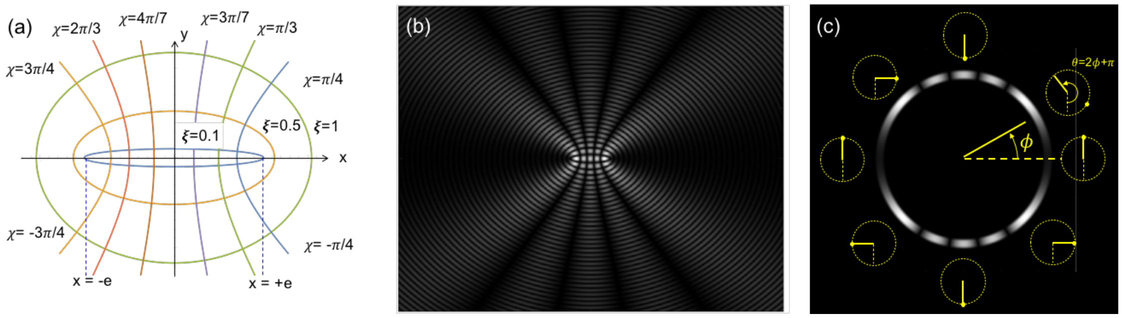

Figure 1. (a) Elliptical coordinates; (b) Mathieu mode with $n = 4$, $q = 30$, even parity; (c) Fourier transform of the mode in (b) showing the correspondence of angles in the Fourier plane (ϕ) and the physical pendulum (θ).

Non-diffracting beams express modes made of plane waves inclined at a constant angle β with the beam axis, and thus with a constant component of the wave-vector along the propagation direction k_z. As a result, the Helmholtz equation reduces to the 2-D Helmholtz equation

$$\frac{\partial^2 U}{\partial x^2} + \frac{\partial^2 U}{\partial y^2} + k_t^2 U = 0\,, \tag{9}$$

where $k_t = k_z \tan\beta \simeq k - k_t^2/(2k)$ is the transverse component of the wave-vector. In elliptical coordinates, Eq. 9 can be separated into the radial and angular equations

$$\frac{d^2 R}{d\xi^2} - (a - 2q\cosh 2\xi)R = 0\,, \tag{10}$$

$$\frac{d^2 \Psi}{d\chi^2} + (a - 2q\cos 2\chi)\Psi = 0\,, \tag{11}$$

respectively, where the second equation can be recognized as the Mathieu equation. Thus, the angular solutions connect with the quantum wave functions of the pendulum. They also obey the relation

$$q = \frac{e^2 k_t^2}{4}\,. \tag{12}$$

Due to the geometry of the pendulum problem, only even eigenvalues of the Mathieu equations correspond to the pendulum solutions.[17,18] The solutions to the problem are given by their parity

$$U(\xi,\chi;q)_{n,e} = \mathrm{ce}_n(\chi;q)\mathrm{Je}_n(\xi;q) \tag{13}$$

for even, and

$$U(\xi,\chi;q)_{n,o} = \mathrm{se}_n(\chi;q)\mathrm{Jo}_n(\xi;q) \tag{14}$$

for odd. The angular solutions with are expressed as

$$\mathrm{ce}_n(\chi;q) = \sum_{k=0}^{\infty} A_k \cos(k\chi), \qquad k \text{ even}, n = 0,2,4,\ldots\,, \tag{15}$$

$$\mathrm{se}_n(\chi;q) = \sum_{k=2}^{\infty} B_k \sin(k\chi), \qquad k \text{ even}, n = 2,4,6,\ldots\,, \tag{16}$$

where A_k and B_k are coefficients. They give rise to even and odd modes with n or $n+1$ hyperbolic nodes, respectively. The radial solutions of the first kind are given by[19]

$$\mathrm{Je}_n(\xi;q) = \frac{\mathrm{ce}_n(0;q)}{A_0} \sum_{k=0}^{\infty} A_k \mathrm{J}_k(2\sqrt{q}\sinh\xi), \qquad k \text{ even}, n = 0,2,4,\ldots\,, \tag{17}$$

$$\mathrm{Jo}_n(\xi;q) = \frac{\mathrm{se}_n'(0;q)}{qB_2}\coth(\xi) \sum_{k=2}^{\infty} kB_k \mathrm{J}_k(2\sqrt{q}\sinh\xi), \qquad k \text{ even}, n = 2,4,6,\ldots\,, \tag{18}$$

where J_k is a Bessel function of order k. The radial solutions have an infinite number of elliptical nodes, but their density depends on q. Figure 1(b) shows an example of a Mathieu mode with $n = 4$, even parity for $q = 30$.

Since the radial functions are expressed in terms of Bessel functions with the same argument, the Fourier transform of a Mathieu mode is a ring modulated by the angular wave function[13]

$$\mathrm{FT}[U_{n,p}(\xi,\chi;q)] = \begin{cases} \mathrm{ce}_n(\theta/2;q)\delta(k-k_t) & p \text{ even} \\ \mathrm{se}_n(\theta/2;q)\delta(k-k_t) & p \text{ odd} \end{cases}, \tag{19}$$

where $\delta(k - k_t)$ is the Dirac delta function. Thus, the light intensity in the Fourier plane is proportional to the quantum-mechanical probability in a 2:1 mapping of the pendulum angle to the beam angle, as shown in Fig. 1(c). The mode also contains the quantum mechanical probability, but spread over the entire mode and distributed in terms of the elliptical angle χ.

In a previous work by our group, we found the measured intensity of a Mathieu mode in the Fourier plane of a lens to be in excellent agreement with the quantum mechanical probability for the corresponding pendulum states.[14,15] We also showed that coherent superpositions of modes were consistent with quantum wavepackets. In particular, we focused on superpositions where the phase between the states was proportional to the energy of the state. We chose the superposition of 4 states, involving even and odd states and two different values of n, of the form

$$U(t) = \frac{1}{2}\left(U_{n,e}e^{-i\varepsilon_{n,e}\tau} + iU_{n,o}e^{-i\varepsilon_{n,o}\tau} + U_{n-2,e}e^{-i\varepsilon_{n-2,e}\tau} + iU_{n-2,o}e^{-i\varepsilon_{n-2,o}\tau}\right), \tag{20}$$

where $\tau = t/(\hbar/E_0)$ is the scaled time with $\hbar$ being the reduced Planck constant. To obtain oscillating wavepacket solutions we added a 90-degree phase between the odd functions and even functions at $\tau = 0$. For energies below the barrier $\varepsilon_{n,e} \neq \varepsilon_{n,o}$, but for states above the barrier $\varepsilon_{n,e} \sim \varepsilon_{n,o}$. We also note that the modes

$$H_n(\xi,\chi;q) = U(\xi,\chi;q)_{n,e} + i\,U(\xi,\chi;q)_{n,o}\,, \tag{21}$$

are known as helical Mathieu modes, which carry orbital angular momentum of $n\hbar$ per photon.[5]

In this article, we investigate a 3-dimensional recreation of this wave-packet. Since the ideal non-diffracting Mathieu beams described by equations 13 and 14 carry infinite energy, they are not realizable in the laboratory, thus we used their finite energy counterpart, the Mathieu-Gauss (MG) beams[20]

$$\mathcal{U}(\mathbf{r})_{n,p} = U_{n,p}(\xi,\chi;q)\,G(\mathbf{r})\,\exp\left(-i\frac{k_t^2}{2k\mu}z\right), \tag{22}$$

with p the parity, $G(\mathbf{r})$ the Gaussian beam

$$G(\mathbf{r}) = \frac{1}{\mu}e^{ikz}\exp\left(-\frac{r^2}{\mu w_0^2}\right), \tag{23}$$

w_0 is the Gaussian beam width, $\mu = 1 + i\frac{z}{z_R}$ and $z_R = kw_0^2/2$ the Rayleigh range. We then generate suitable superpositions of these beams where the z coordinate plays the role of time, and so the mode will change in 3-D following the dynamics of the corresponding quantum wavepacket. In particular, the spatial wave packet is given by

$$\mathrm{U}(\mathbf{r})_= [H(\xi,\chi;q)_{n_1}\,G(\mathbf{r})]\;e^{-i\alpha(k_{t_1})z} + [H(\xi,\chi;q)_{n_2}\,G(\mathbf{r})]\;e^{-i\alpha(k_{t_2})z}\,, \tag{24}$$

with

$$\alpha(k_t) = \frac{k_t^2}{2k\mu}\,, \tag{25}$$

and which we have written in a convenient manner, so the analogy to the quantum states is more evident. Thus, we aim to prepare beams with $\alpha(k_t)$ proportional to the energy of each state. This is possible by changing k_t and e in Eq. 12 so that q remains constant for all modes in the superposition.

3. EXPERIMENTAL PROCEDURE

A schematic of the apparatus is shown in Fig. 2. The output of a helium-neon laser is expanded and sent to a reflective spatial light modulator (SLM), which modulates the light according to the encoded optical mode into the first diffraction order. We use a 4-f system of lenses to relay the mode and its Fourier transform, which are imaged by digital cameras. A beam splitter allows simultaneous imaging of the mode and its Fourier transform. The camera that images the beam mode is translated along a track to record its shape along the propagation direction.

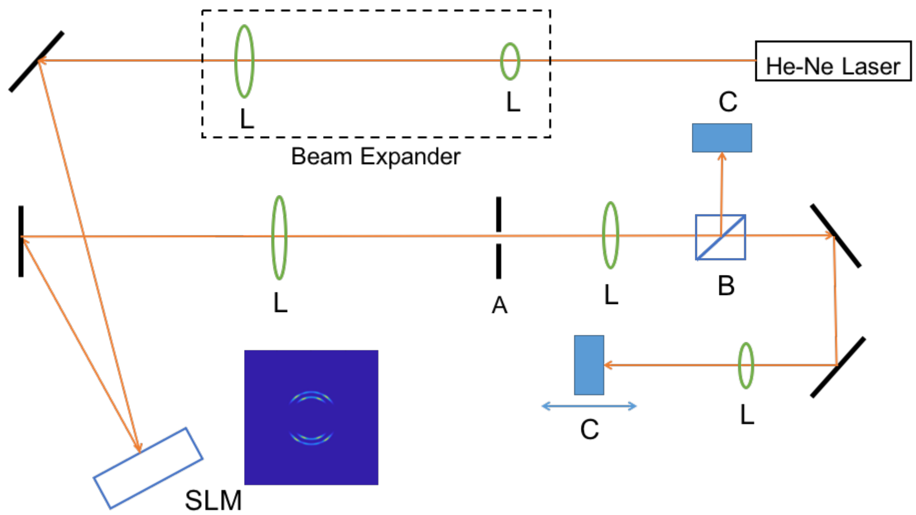

Figure 2. Schematic of the apparatus, which includes a spatial light modulator (SLM), lenses (L), and aperture (A) a beam splitter (B) and cameras (C) The insert shows the pattern programmed onto the SLM.

The method presented in this article involves programming the SLM with the Fourier transform of the desired mode superposition (Eq. 24 with $z = 0$). To implement the latter, we first calculated numerically the individual helical modes using the Mathieu functions as described by Gutierrez-Vega,[19] then numerically propagated them to the back focal plane of a thin lens,[21] and finally added them together to obtained the total mode to be encoded in the SLM. The hologram was created using complex amplitude modulation[22] following standard light shaping techniques,[23] including a linear phase grating, to separate our mode from the zero-order un-modulated light, and a calibration matrix to counteract the aberrations of the optical system.

Crucially, each helical mode in the superposition has a distinct value of k_t, so their Fourier transforms correspond to rings of different diameter. This is clearly seen in Figure 3, where we present the mode intensity and phase, as well as its corresponding hologram for two examples of the superpositions we studied. The holograms are shown without the linear grating and correction matrix for the sake of better visualization. In addition, notice the ring width is finite, as opposed to the infinitesimally thin ring of Eq. 19. This arises from the Gaussian term in the Mathieu-Gauss modes, in such a way the larger w_0 the thinner the ring is, since in such cases we are approaching the ideal non-diffracting Mathieu beams.

Notice that since there is a 2:1 relation between the pendulum angle and the mode angular variable via Eq. 2, one full revolution of the pendulum corresponds to half a revolution of the pattern at the Fourier plane. Thus, defining the polar angle of the Fourier patterns by ϕ, as shown in Fig. 1(c), with $\phi = 0, \pi$ corresponding to the pendulum bob at the inverted position, and $\phi = \pi/2, -\pi/2$ to its resting position. If the Fourier pattern is non zero at $\phi = 0, \pi$, as in Fig. 3(a), it means that the probability of finding the pendulum at the inverted position is non zero. Conversely, if the pattern is zero at $\phi = 0, \pi$, as in Fig. 3(b) (and Fig 1(c)), it represents an oscillating state of the pendulum, with the closest angle to $\phi = 0, \pi$ with non-zero intensity corresponding to the turning point of the pendulum oscillation.[14]

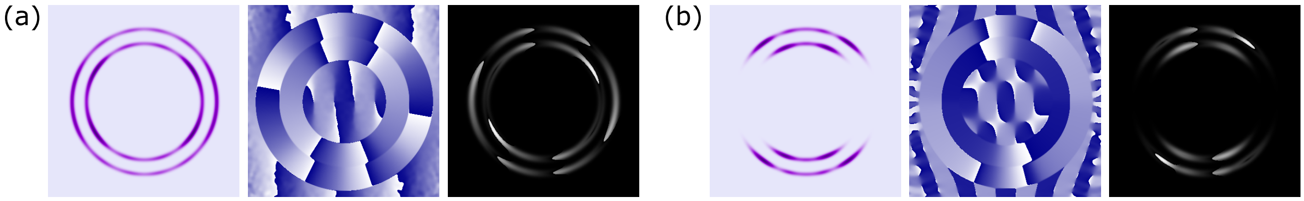

Figure 3. Example of the programming of the Fourier transform of the superpositions of helical Mathieu-Gauss modes with $w_0 = 1 \times 10^{-3}$ m for: (a) $k_{t_1} 5 \times 10^4$ m^{-1}, $e_1 = 1.5 \times 10^{-4}$ m, $n_1 = 6$; $k_{t_2} = 4 \times 10^4$ m^{-1}, $e_2 = 1.9 \times 10^{-4}$ m and $n_2 = 4$; and (b) $k_{t_1} = 5 \times 10^4$ m^{-1}, $e_1 = 3 \times 10^{-4}$ m, $n_1 = 4$; $k_{t_2} = 4 \times 10^4$ m^{-1}, $e_2 = 3.8 \times 10^{-4}$ m and $n_2 = 2$. In each case the superposition intensity, phase and corresponding hologram are shown to the left, middle and right, respectively.

4. EXPERIMENTAL RESULTS

In a first attempt at producing experimental results, we made some compromises. One involves assuming that the energies of the even and odd states are equal (i.e. $\varepsilon_{n,e} \sim \varepsilon_{n,o}$). This is true only for unbounded quantum states, which are above the potential barrier (i.e., $\varepsilon_n > q$).[14] The second was to use convenient values of k_t. They correspond to values of $\alpha(k_t)$ that do not always correspond exactly to the energies of the pendulum states. However, this only affected the rate of evolution of the relative phase with z, but not the dynamics itself.

Figure 4 shows three cases of superpositions of four unbounded states. Case-I, shown in panes (a)-(e) correspond to $n_1 = 6$, $n_2 = 4$ and $q = 3.5$, for which the states have energies well above the pendulum potential barrier: $\varepsilon_6 = 2.8q$ and $\varepsilon_4 = 1.5q$. Case-II, shown in panes (f)-(j), correspond to $n_1 = 6$, $n_2 = 4$ and $q = 14.1$, resulting in one energy level slightly above the barrier ($\varepsilon_6 = 1.2q$) and the other slightly below ($\varepsilon_4 = 0.94q$). Case-III corresponds to $n_1 = 4$, $n_2 = 2$ and $q = 56$, shown in panes (k)-(o), in which the energy of both states is well below the barrier: $\varepsilon_4 = 0.3q$ and $\varepsilon_2 = 0.14q$.

We can observe the differences in energies in the measured Fourier patterns (a), (f) and (k), as explained in the previous section. In case-I (Fig. 4(a)) the two rings are completely closed, in case-II (Fig. 4(f)) one is closed and the other has a minimum at the inverted position of the pendulum (i.e., $\phi = 0, \pi$), and in case-III both levels appear as arcs.

As mentioned earlier, the mode patterns also display the quantum-mechanical information but spread throughout the mode and specified by the elliptical-angular variable χ. The patterns also show two periods of the pendulum due to Eq. 2. With this in mind, we observe that the angular intensity pattern for case-I rotates as a function of the propagation distance z, which is proportional to time. The pattern represents a wavepacket that behaves like a pendulum rotor. In case-II, we still see rotation, but also containing nodes, looking like "teeth," which are typical of bound states.[14,15] The pattern shows the evolution dynamics of the quantum picture: a probability featuring nodes that also rotate as the beam propagates. The patterns in case-III show some sloshing of the intensity, which could be correlated with oscillations: the intensity shifts from one turning point to the other. We expect that these dynamics will become clearer when the individual energies of the states of same-n but different parity are used.

5. DISCUSSION AND CONCLUSIONS

As shown in this article, we prepared light beams in non-difracting pendulum modes with propagation constants that make them accumulate a varying phase upon propagation. The evolution of the mode shape along the physical propagation dimension mimics the temporal evolution of a pendulum quantum wavepacket. The measurements of pendulum-mode superpositions reproduce well the temporal dynamics of a pendulum rotor. Similarly, we see promising results in the preparation of librating wavepacket modes. We are in the process of refining our measurements to reproduce the spatial wavepackets that correspond to the quantum pendulum. This work underscores the value of non-diffracting beams in the generation of optical beams that display complex patterns in space, and which simulate a very distinct physical system such as the quantum pendulum.

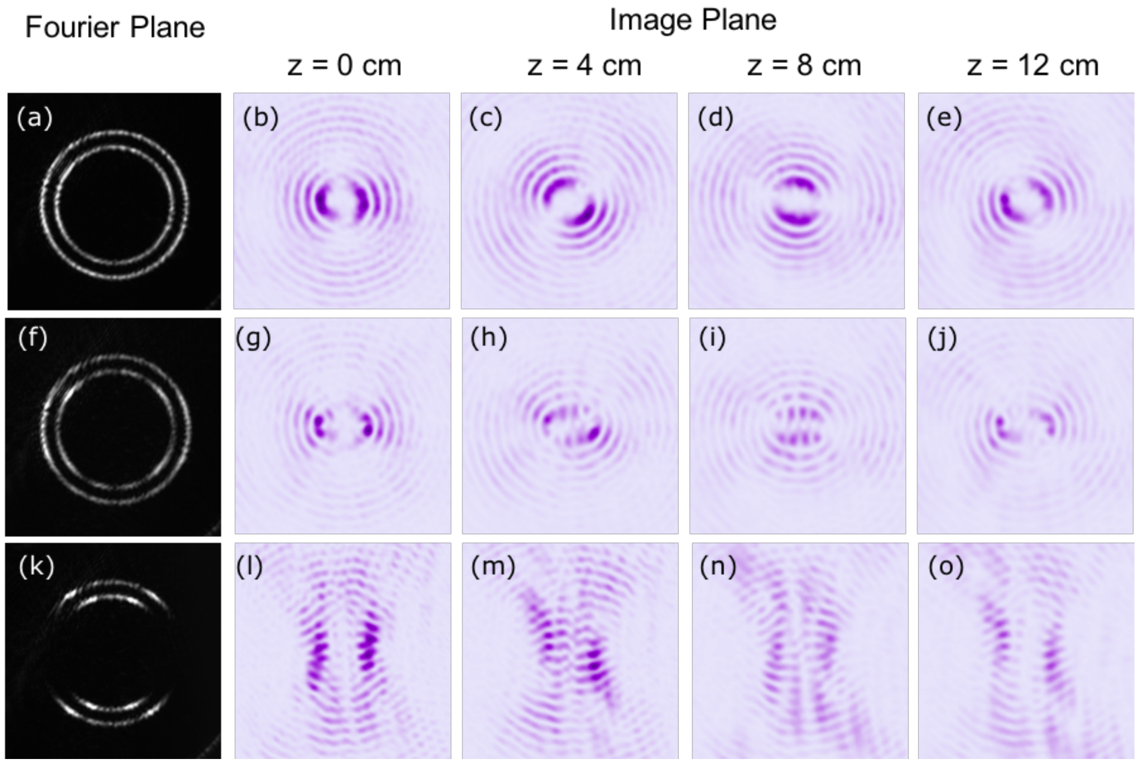

Figure 4. Measurements of mode superpositions of helical Mathieu-Gauss modes for three cases. In case-I (a)-(e) $q = 3.5$, $k_{t_1} = 5 \times 10^4$ m^{-1}, $e_1 = 7.5 \times 10^{-5}$ m, $n_1 = 6$, $k_{t_2} = 4 \times 10^4$ m^{-1}, $e_2 = 9.4 \times 10^{-4}$ m and $n_2 = 4$, which correspond to the unbound pendulum rotor. In case-II (f)-(j) $q = 14.1$, $k_{t_1} = 5 \times 10^4$ m^{-1}, $e_1 = 1.5 \times 10^{-4}$ m, $n_1 = 6$, $k_{t_2} = 4 \times 10^4$ m^{-1}, $e_2 = 1.9 \times 10^{-4}$ m and $n_2 = 4$, which is an intermediate case between bound librator and unbound rotor. In case-III (k)-(o) $q = 56$, $k_{t_1} = 5 \times 10^4$ m^{-1}, $e_1 = 3 \times 10^{-4}$ m, $n_1 = 4$, $k_{t_2} = 4 \times 10^4$ m^{-1}, $e_2 = 3.8 \times 10^{-4}$ m and $n_2 = 2$ that correspond to the bound pendulum librator. Panes (a) and, (f) and (k) show the measured Fourier pattern of the superposition, and panes (b)-(e), (g)-(j) and (l)-(o) show the image of the modes for different propagation distances z.

ACKNOWLEDGMENTS

This work was supported by National Science Foundation grant PHY-2011937. We thank J.M Freedman, F.J. Auccapuclla and Y. Qin for early work on this problem.

REFERENCES

[1] M. Marte and S. Stenholm, "Paraxial light and atom optics: The optical Schrödinger equation and beyond," *Phys. Rev. A* **56**, pp. 2940–2953, 1997.

[2] J. Durnin, J. J. Miceli, and J. H. Eberly, "Diffraction-free beams," *Phys. Rev. Lett.* **58**, pp. 1499–1501, Apr 1987.

[3] J. Durnin, "Exact solutions for nondiffracting beams. i. the scalar theory," *J. Opt. Soc. Am. A* **4**(4), pp. 651–654, 1987.

[4] J. Gutiérrez-Vega, M. Iturbe-Castillo, and S. Chávez-Cerda, "Alternative formulation for invariant optical fields: Mathieu beams," *Opt. Lett.* **25**, pp. 1493–1495, 2000.

[5] J. Gutiérrez-Vega, M. Iturbe-Castillo, G. Ramírez, E. Tepichín, R. Rodríguez-Dagnino, S. Chávez-Cerda, and G. New, "Experimental demonstration of Mathieu beams," *Opt. Commun.* **195**, pp. 35–40, 2001.

[6] M. V. Berry and N. L. Balazs, "Nonspreading wave packets," *Am. J. Phys.* **47**, pp. 264–267, 1979.

[7] G. A. Siviloglou, J. Broky, A. Dogariu, and D. N. Christodoulides, "Observation of accelerating airy beams," *Phys. Rev. Lett.* **99**, p. 213901, Nov 2007.

[8] M. A. Bandres, J. C. Gutiérrez-Vega, and S. Chávez-Cerda, "Parabolic nondiffracting optical wave fields," *Opt. Lett.* **29**, pp. 44–46, 2004.

[9] A. Zannotti, C. Denz, M. Alonso, and M. Dennis, "Shaping caustics into propagation-invariant light," *Nat. Comm.* **11**, p. 3597, 2020.

[10] N. Efremidis and D. Christodoulides, "Abruptly autofocusing waves," *Opt. Lett.* **35**, pp. 4045–4047, 2010.

[11] J. D. Ring, J. Lindberg, A. Mourka, M. Mazilu, K. Dholakia, and M. R. Dennis, "Auto-focusing and self-healing of pearcey beams," *Opt. Express* **20**(17), pp. 18955–18966, 2012.

[12] C. Schulze, F. S. Roux, A. Dudley, R. Rop, M. Duparré, and A. Forbes, "Accelerated rotation with orbital angular momentum modes," *Phys. Rev. A* **91**, p. 043821, 2015.

[13] M. Dennis and J. Ring, "Propagation-invariant beams with quantum pendulum spectra: from Bessel beams to Gaussian beam-beams," *Opt. Lett.* **38**, pp. 3325–3328, 2013.

[14] E. Galvez, F. Auccapuclla, K. Wittler, and Y. Qin, "Pendulum beams: A window into the quantum pendulum," *Proc. SPIE* **10935**, p. 1093509, 2019.

[15] E. Galvez, F. Auccapuclla, Y. Qin, K. Wittler, and J. Freedman, "Pendulum beams: optical modes that simulate the quantum pendulum," *J. Opt.* **23**, p. 024001, 2021.

[16] E. Condon, "The physical pendulum in quantum mechanics," *Phys. Rev.* **31**, pp. 891–894, 1928.

[17] G. Baker, J. Blackburn, and H. Smith, "The quantum pendulum: Small and large," *Am. J. Phys.* **70**, pp. 525–531, 2002.

[18] J. Gutiérrez-Vega, R. Rodríguez-Dagnino, M. Meneses-Nava, and S. Chávez-Cerda, "Mathieu functions, a visual approach," *Am. J. Phys.* **71**, pp. 233–242, 2003.

[19] J. Gutierrez-Vega, *Formal analysis of the propagation of invariant optical fields in elliptic coordinates.* PhD thesis, INAOE, Mexico, 2000.

[20] J. C. Gutiérrez-Vega and M. A. Bandres, "Helmholtz–Gauss waves," *Journal of the Optical Society of America A* **22**, p. 289, feb 2005.

[21] D. G. Voelz, *Computational fourier optics: a MATLAB tutorial*, SPIE press Bellingham, WA, 2011.

[22] E. Bolduc, N. Bent, E. Santamato, E. Karimi, and R. W. Boyd, "Exact solution to simultaneous intensity and phase encryption with a single phase-only hologram," *Opt. Lett.* **38**(18), pp. 3546–3549, 2013.

[23] C. Rosales-Guzmán and A. Forbes, *How to shape light with spatial light modulators*, SPIE Press, 2017.